

# Computer simulation studies of aqueous solutions at ambient and supercritical conditions using effective pair potential and polarizable potential models for water

S. Koneshan<sup>a)</sup> and Jayendran C. Rasaiah  
*Department of Chemistry, University of Maine, Orono, Maine 04469*

Liem X. Dang  
*Pacific Northwest National Laboratory, P.O. Box 999, Mail Stop K8-91, Richland, Washington 99352*

(Received 31 October 2000; accepted 29 December 2000)

This paper discusses the computer simulation of the diffusion coefficients and structure of infinitely dilute aqueous ionic solutions at ambient (298 K, solvent density  $0.997 \text{ g cm}^{-3}$ ) and supercritical (683 K, solvent density  $0.35 \text{ g cm}^{-3}$ ) conditions using two different models for water. They are the extended simple point charge (SPC/E) and renormalized polarizability (RPOL) models in which the electronic polarizations of the water molecule are treated differently. The effect of polarizability is implicit in the SPC/E model and explicit in the RPOL model. The RPOL model shows slightly greater hydrogen bonding, at room temperature than the SPC/E model, but less hydrogen bonding at 683 K. It is concluded that the explicit neglect of electronic polarization of the solvent and ions in calculations based on the SPC/E model of water, has only a small effect on the diffusion coefficients of the ions. Both models predict diffusion coefficients of ions in supercritical water that are weakly dependent on their size in contrast to their behavior under ambient conditions discussed in previous work [S. Koneshan *et al.*, *J. Phys. Chem.* **102**, 4193 (1998)]. The simulations suggest that the mechanism of diffusion at the ambient and supercritical states of the solvent water is different. © 2001 American Institute of Physics. [DOI: 10.1063/1.1350447]

## I. INTRODUCTION

The effects of electronic polarization on the structure and dynamics of ions in aqueous solution are not completely understood, although model potentials and tools to investigate this by molecular dynamics simulation have been available for some time. This paper discusses the simulation of the diffusion coefficients and structure of infinitely dilute aqueous ionic solutions at ambient and supercritical conditions using two different models for water, namely the SPC/E and RPOL models in which the polarizability of the water molecule is treated differently. The polarizability of the ions is also considered in our calculations of the structure and dynamics of  $\text{Na}^+$ ,  $\text{Cl}^-$ ,  $\text{Li}^+$ , and  $\text{F}^-$  ions using the RPOL model for water. The relevant potentials for the interactions between ions and water in the two models (SPC/E and RPOL) are available in the literature from the work of Dang and his group, who fitted the potential parameters to the hydration energies of small ion-water clusters.<sup>1,2</sup> This provides an opportunity to determine whether calculations of solvation thermodynamics<sup>3</sup> and ion mobility in aqueous solutions at ambient<sup>4-6</sup> and supercritical temperatures,<sup>7-10</sup> using the SPC/E model for water, are seriously compromised by the complete neglect of ion polarizability and the approximate treatment of solvent polarizability and its temperature dependence.

The water molecule in the SPC/E model is treated as a

collection of point charges distributed over the atomic sites with Lennard-Jones interactions between the oxygen atoms.<sup>11</sup> The model was developed from the simple point charged (SPC) model, to account for the effect of the polarizability of the water molecule at ambient conditions in an approximate way by reparametrizing the charges and non-bonded Lennard-Jones interactions. The effective dipole moment of water in this model is 2.35 Debye, in contrast to the dipole moment of an isolated water molecule which is 1.85 Debye. The SPC/E model has been used extensively in computer simulation studies of the thermodynamic and transport properties of ions and uncharged solutes during the past few years.<sup>3-10</sup> The ion diffusion coefficients calculated from this model are found to show the same trends with respect to ion size as experimental results at room temperature, with distinct curves and maxima for positive and negative ions when the mobility is plotted as a function of size.<sup>5,4</sup> These calculations have been extended recently to the study of ions and uncharged solutes at supercritical temperatures using the same SPC/E model for water.<sup>7-10</sup>

However, one problem in modeling supercritical aqueous solutions with the SPC or SPC/E models lies in the significant amount of hydrogen bonding implicit in point charge models with parameters fitted to ambient conditions. Neutron diffraction experiments with isotopic substitution<sup>12</sup> (NDIS) suggest a decrease in hydrogen bonding with rise in temperature based on the reduction in the height of the hydrogen bonding peak at  $1.2 \text{ \AA}$ , in the O-H radial distribution function. Intuitively this reduction in hydrogen bonding seems very reasonable. However, the failure of the simple point

<sup>a)</sup>Current address: Department of Computer Science, Upson Hall, Cornell University, Ithaca, New York.

charge models parametrized at room temperature to account for this reduction, can be traced to changes in the effective dipole and multipole moments of water when the temperature shifts from ambient to supercritical conditions, but are constant in these models. The magnitude of these effects are unknown, and this raises the question whether calculations of the diffusion coefficients and conductivity of ions at high temperatures using the SPC/E model for water,<sup>4–8</sup> contain significant errors due to the neglect or approximate treatment of electronic polarization of the water molecule. A related question is whether the polarization of ions in real aqueous solutions also has a significant effect on the transport properties of simple monovalent ions between temperatures and densities characteristic of ambient conditions and the supercritical region.

Effects due to the polarizability of water have been handled in the past by changing the effective dipole moment as a function of temperature. The resulting structural and thermodynamic properties show the correct trends including a decrease in the hydrogen bonding peak at 1.2 Å in the O–H radial distribution function. However the O–H and O–O radial distribution functions do not exactly coincide with observed NDIS results.<sup>13</sup>

Dang incorporated oxygen and hydrogen atom polarization in water by adopting a three-site polarization model<sup>2</sup> that eventually developed into the renormalized polarization (RPOL) model for water. Thus in the RPOL model, the polarization of the oxygen and hydrogen atoms are treated explicitly. The SPC/E and RPOL models also have a significant amount of charge asymmetry that differentiates between the solvation of positive and negative ions of the same size and charge magnitude. The oxygen atom of a water molecule in the primary hydration shell of a cation is closer to the ion than the hydrogen atoms of the same water molecule, whereas an anion has one of the hydrogen atoms of the water molecules nearest to it. Reversing the charge of an ion breaks the symmetry of the ion water interaction.

Smith and Dang<sup>14</sup> investigated the thermodynamics and kinetics of NaCl association using the RPOL model for water and found that the effect of polarization is small but measurable. In this paper we investigate the effect of polarization on the diffusion of ions and the structure of water molecules in the primary hydration spheres of simple monovalent ions (Na<sup>+</sup>, Cl<sup>−</sup>, Li<sup>+</sup>, and F<sup>−</sup>) using the SPC/E and RPOL models for water at ambient and supercritical temperatures. Our studies thus provide information on the effect of polarization on the structure and dynamics of ions under widely different conditions of temperature and solvent density. This includes the supercritical region characterized by voids and spatial and temporal fluctuations in the density that give rise to interesting chemical and physical properties.<sup>15–20</sup>

There have been many other studies of polarizable water models. Mountain<sup>21</sup> compared fixed charged and polarizable models for water with the Stillinger–Rahman ST2 (fixed charge) and RPOL (polarizable) interatomic potential functions, respectively. There were no ions present in the system, and it was found that the explicit inclusion of polarization had only a small effect on the pair correlation functions of water for the temperatures and densities examined, which are

comparable to those used in this study. Yoshii *et al.*<sup>22</sup> investigated structural changes on passing from subcritical to supercritical temperatures by molecular dynamics simulations of the RPOL model for water. Several others have also studied various polarizable molecular models for water<sup>23,24</sup> over the last decade, while *ab initio* molecular dynamics methods have been employed more recently by a small but growing number of investigators.<sup>25,26</sup> Kim and co-workers<sup>27</sup> have carried out MD simulations of ambient and supercritical water in which the electronic wave function and polarizability are represented with a truncated adiabatic basis set (TAB).

The treatment of the electronic polarization of water and ions can be computationally demanding, especially when *ab initio* MD calculations are employed or even at the simpler level of polarizable molecular models. It is clearly important to know under what circumstances electronic polarization effects are dominant in the neat liquid and in solutions. Our study seeks to address this question directly, by determining the influence of electronic polarization on the structure and dynamics of infinitely dilute ionic solutions at ambient and supercritical temperatures. We do this by explicit comparison of the properties of a representative set of ions using the SPC/E and RPOL models for water with ion–water potential parameters fitted to the hydration energies of small ion–water clusters.<sup>1,2</sup>

## II. INTERACTION MODELS AND SIMULATION DETAILS

The SPC/E and RPOL models were used throughout this molecular dynamics study of selected ions (Na<sup>+</sup>, Cl<sup>−</sup>, Li<sup>+</sup>, and F<sup>−</sup>) at infinite dilution in water at 298 K and at 683 K at different solvent densities. In the SPC/E model of water the OH bond distances are constrained at 1.0 Å. The bond angle between the two OH bonds is fixed at 109.47°. The intermolecular interaction between a pair of water molecules is

$$u_{\text{pair}} = 4\epsilon_{\text{OO}} \left[ \left( \frac{\sigma_{\text{OO}}}{r_{\text{OO}}} \right)^{12} - \left( \frac{\sigma_{\text{OO}}}{r_{\text{OO}}} \right)^6 \right] + \frac{1}{4\pi\epsilon_0} \sum_{i=1}^3 \sum_{j=1}^3 \frac{q_i q_j}{r_{ij}}. \quad (2.1)$$

The first term is the Lennard-Jones potential energy of interaction evaluated between the oxygen sites on distinct water molecules and the second term is the sum of electrostatic potential energies of interaction between the charges on sites *i* and *j* of distinct molecules. Here  $q_i$  is the charge on site *i* and  $r_{ij}$  is the distance between the sites *i* and *j*.

In the RPOL model, there are dipoles in addition to the point charges at each atomic site, and the intermolecular interaction between a pair of water molecules is given by

$$U_{\text{tot}} = U_{\text{pair}} + U_{\text{pol}}, \quad (2.2)$$

where

$$U_{\text{pol}} = -\frac{1}{2} \sum_{i=1}^2 \vec{\mu}_i \cdot \vec{E}_i^0 \quad (2.3)$$

with

$$\vec{\mu}_i = \alpha_i \vec{E}_i, \quad (2.4)$$

TABLE I. Interaction parameters for the SPC/E model.

Ion/water	$\sigma_{iO}(\text{\AA})$	$\epsilon_{iO}(\text{kJ/mol})$	Charge ( $q$ )
Li <sup>+</sup>	2.337	0.6700	+1
Na <sup>+</sup>	2.876	0.5216	+1
F <sup>-</sup>	3.143	0.6998	-1
Cl <sup>-</sup>	3.785	0.5216	-1
SPC/E	$\sigma_{OO}(\text{\AA})$	$\epsilon_{OO}(\text{kJ/mol})$	Charge ( $q$ )
O(H <sub>2</sub> O)	3.169	0.6502	-0.8476
H(H <sub>2</sub> O)			+0.4238

$$\vec{E}_i = \vec{E}_i^0 + \sum_{j=1, j \neq i} \vec{T}_{ij} \cdot \vec{\mu}_j, \quad (2.5)$$

$$E_i^0 = \sum_{j=1, j \neq i} \frac{q_j \vec{r}_{ij}}{r_{ij}^3}, \quad (2.6)$$

and

$$\vec{T}_{ij} = \frac{1}{r_{ij}^3} \left( \frac{3\vec{r}_{ij}\vec{r}_{ij}}{r_{ij}^2} - \vec{I} \right). \quad (2.7)$$

$\vec{T}_{ij}$  is the dipole-dipole tensor,  $\alpha_i$  is the polarizability of atom  $i$ ,  $\vec{r}_{ij}$  is the vector from atom  $i$  to atom  $j$ , and  $q_j$  is the charge on atom  $j$ . The parameters for the ion-water and water-water interactions are summarized in Table I and Table II for the SPC/E and RPOL water models, respectively. The potential parameters for the ion-water interactions were fitted by Dang and his group to the hydration energies of small ion-water clusters.<sup>1,2</sup> In our studies of ions at infinite dilution, only water molecules surround each ion. The electric field at the surface of an ion, due to its charge, decreases as the square of its radius, while the polarizability of an ion increases substantially with its size as seen in Table II.

*Simulation of bulk water and of a single ion at infinite dilution using the RPOL and SPC/E models for water.* The critical density and temperature of water are 0.32 g cm<sup>-3</sup> and 647 K, respectively, while the density at 298 K is nearly 0.997 g cm<sup>-3</sup>. Our simulations were carried out in the NVT ensemble for two states; in one state the density of water in a cubic box of length 26.3879 Å was 0.35 g cm<sup>-3</sup> with the temperature set at 683 K. This is in the supercritical region of water. In the other state, the water density in a cubic box of length 18.64 Å was 0.997 g cm<sup>-3</sup> and the temperature was controlled at 298 K. The number of water molecules in each

TABLE II. Interaction parameters for the RPOL model.

Ion	$\sigma_{iO}(\text{\AA})$	$\epsilon_{iO}(\text{kJ/mol})$	Charge ( $q$ )	$\alpha(\text{\AA}^3)$
Li <sup>+</sup>	2.351	0.6798	+1	0.029
Na <sup>+</sup>	2.773	0.6034	+1	0.240
F <sup>-</sup>	3.182	0.7485	-1	0.974
Cl <sup>-</sup>	3.823	0.5292	-1	3.250
RPOL	$\sigma_{OO}(\text{\AA})$	$\epsilon_{OO}(\text{kJ/mol})$	Charge ( $q$ )	$\alpha(\text{\AA}^3)$
O(H <sub>2</sub> O)	3.196	0.6694	-0.730	0.528
H(H <sub>2</sub> O)			+0.365	0.170

box was 216 and a time step of 1 femtosecond was used in the simulations. The systems were equilibrated over 20 000 time steps corresponding to an equilibration time of 20 ps. The production runs consisted of another 20 000 time steps after equilibrium. The simulations of an ion in water required longer equilibration times of over 250 000 time steps (250 ps) and production runs for another 250 000 time steps after equilibration. In this case, we used a system consisting of a single solute and 215 water molecules in the NVT ensemble, at a solvent density of 0.350 g cm<sup>-3</sup> at 683 K and 0.997 g cm<sup>-3</sup> at 298 K. During the simulation, the induced dipole moment  $\mu_i$  and the electrostatic field  $E_i$  at the polarization center are evaluated by a self-consistent method. Equations (2.4) and (2.5) were solved iteratively until the root mean square of the difference in the induced-dipole moment in successive iterations was less than 0.01 D/atom. In all cases a reaction field correction was used to account for the long-range Coulomb interactions between the charges. The correction term for the Coulomb interaction energy between atomic sites  $i$  and  $j$  is

$$\frac{q_i q_j}{r_{ij}} \left\{ \left( \frac{\epsilon_{RF} - 1}{2\epsilon_{RF} + 1} \right) \frac{r_{ij}^3}{R_c^3} \right\}. \quad (2.8)$$

Here  $\epsilon_{RF}$  is the dielectric constant of the medium surrounding the cutoff sphere of radius  $R_c$ , which is half the length of the simulation box. In Eq. (2.8), the values of  $\epsilon_{RF}$  at 298 K and 683 K were fixed at 22.0 and 5.0, respectively. The temperature was controlled at 298 K and a quaternion formulation was employed to solve the equations of rotational motion about the center of mass of rigid SPC/E and RPOL water molecules. A fifth order predictor corrector algorithm with a time step of 1 fs was used to integrate the equations of motion.

### III. RESULTS

*Distribution functions and hydrogen bonding in the RPOL model for water.* Our simulations at 683 K of the RPOL model for water show a significant decrease in the hydrogen bonding peak of the oxygen-hydrogen radial distribution function at 1.9 Å in contrast to the results for the SPC/E model (see Fig. 1 below). This effect, which is also observed in neutron scattering experiments (NDIS), indicates that polarization may play an important role in determining the structure of water in the bulk and near an ion at elevated temperatures.

The coordination numbers for the two models are nearly the same for the SPC/E and RPOL models, respectively, at 683 K, and 298 K.

To investigate the effect of hydrogen bonding further we follow Luzar and Chandler.<sup>28,29</sup> A pair of water molecules is hydrogen bonded when the following criteria are satisfied.

- The interoxygen distance is less than the distance equal to the position of the first minimum in the oxygen-oxygen distribution function.
- The O-H distance between the bonded molecules is less than the corresponding distance to the first minimum in the oxygen-hydrogen distribution function.

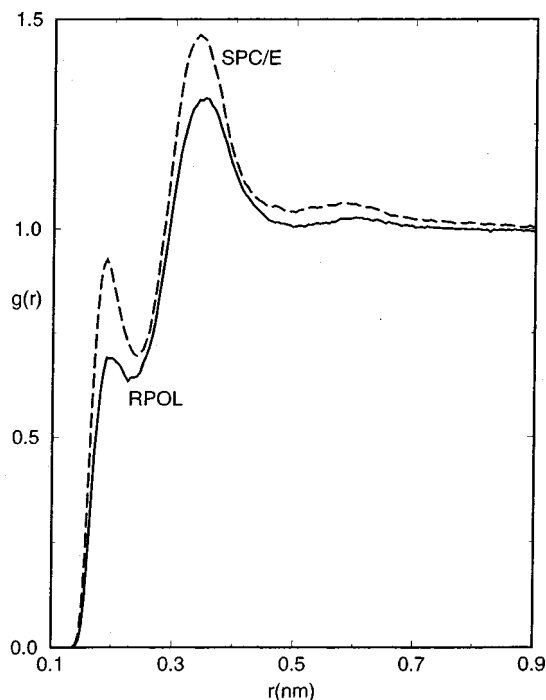


FIG. 1. O–H radial distribution function of SPC/E (dashed line) and RPOL (full line) water at 683 K at a water density of  $0.350 \text{ g/cm}^3$ . Note that the hydrogen bonding peak at  $0.19 \text{ nm}$  of RPOL water is significantly lower than that of the SPC/E water.

- (c) The O–H–O angle is less than  $30^\circ$ . The critical distances for two different water models, are collected in Table III.

Luzar and Chandler define a hydrogen-bond population operator  $h(t)$ , as one if a pair of water molecules is hydrogen bonded and zero otherwise. The persistence of hydrogen bonding is measured by the time correlation function

$$c(t) = \frac{\langle h(t)h(0) \rangle}{\langle h \rangle} \quad (3.1)$$

Here  $\langle h \rangle$  is the time average of  $h$ ; the number of intermolecular hydrogen bonds in a water molecule. We use the  $c(t)$  functions shown in Fig. 2 as a measure of the persistence of hydrogen bonding between two  $h$ -bonded water molecules in the SPC/E and RPOL models at the two state points corresponding to 298 K and 683 K.

By this criterion, the RPOL model shows slightly greater hydrogen bonding, at room temperature than the SPC/E model but less hydrogen bonding (as shown in Fig. 2) at 683 K

TABLE III. Oxygen–oxygen and oxygen–hydrogen distribution functions for SPC/E and RPOL water at 298 K and density of  $0.997 \text{ g cm}^{-3}$  and 683 K at a density of  $0.35 \text{ g cm}^{-3}$  for the SPC/E and RPOL models.

Mode (temp)	First minimum RDF		Angle O–H–O
	$R_{\text{OO}}(\text{\AA})$	$R_{\text{OH}}(\text{\AA})$	
SPC/E (298 K)	3.34	2.37	30
RPOL (298 K)	3.29	2.36	30
SPC/E (683 K)	4.24	2.40	30
RPOL (683 K)	4.51	2.25	30

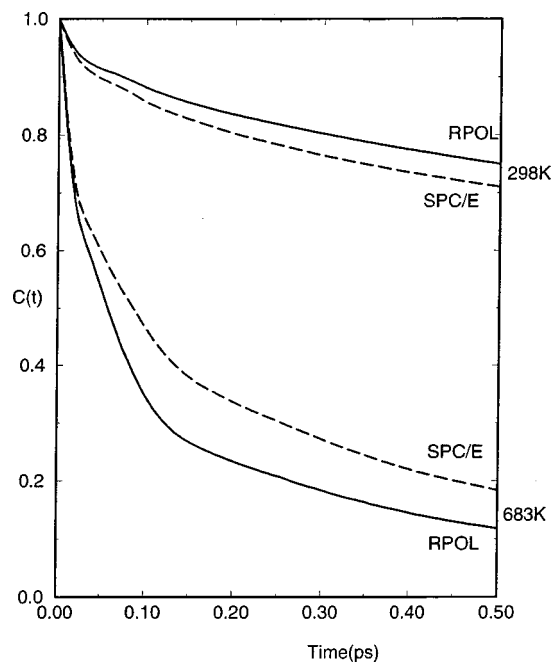


FIG. 2. The hydrogen-bond correlation function  $C(t)$  given by Eq. (3.1) at 298 K ( $0.997 \text{ g/cm}^3$ ) and 683 K ( $0.350 \text{ g/cm}^3$ ) for both SPC/E (dashed line) and RPOL (full line) models. At 298 K, RPOL model shows greater persistence of hydrogen bonding than the SPC/E model but at 683 K, the opposite is observed.

K. This shows that the atomic polarization in the RPOL model does indeed lead to an adjustment of the total dipole moment of the water molecule that depends on its interaction with the surrounding environment. It is reflected in the temperature and density dependence of hydrogen bonding in the RPOL model for water which is more realistic in this respect than the SPC/E model for water.

#### IV. THE DIFFUSION COEFFICIENT OF WATER

The diffusion coefficients  $D$  of RPOL and SPC/E water were calculated from mean square displacements (MSD) in the usual way using the relation

$$D = \frac{1}{6} \lim_{t \rightarrow \infty} \frac{d}{dt} \langle |\vec{r}(t) - \vec{r}(0)|^2 \rangle. \quad (4.1)$$

Figure 3 compares the MSD of RPOL and SPC/E water at 683 K obtained in our simulations. Examination of this figure reveals that the change in the slope of the mean square displacement between the RPOL and SPC/E models is small. As a result the diffusion coefficient, which is  $1/6$  the slope of the mean square displacement curve, is very nearly the same for the two models. This indicates that the effect of atomic polarization on the diffusion of water represented by this model is small at elevated temperatures. It should be borne in mind however, that the density of water studied at 683 K is about one-third the density of water under ambient conditions, and the low density may also contribute to the small effect that polarizability has on the diffusion coefficients of water.

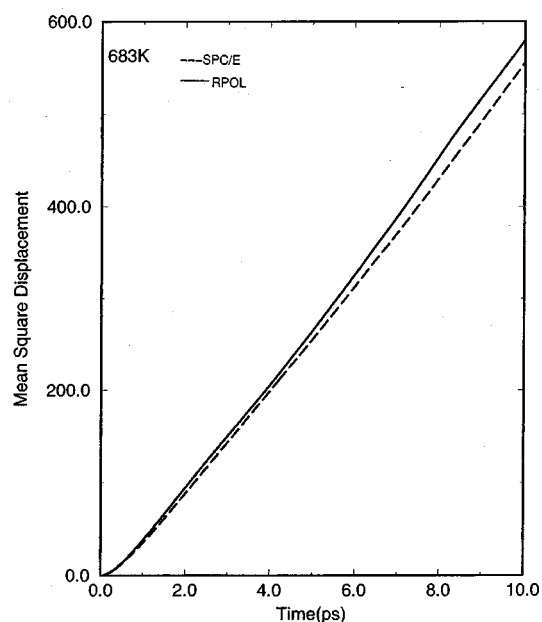


FIG. 3. Comparison between the mean square displacements in  $\text{\AA}^2$  of SPC/E (dashed line) and RPOL (full line) water as a function of the time in picoseconds. The density of water is  $0.35 \text{ g cm}^{-3}$  and temperature 683 K.

The velocity autocorrelation function  $\langle \mathbf{v}(t) \cdot \mathbf{v}(0) \rangle$ , can also be used to calculate the diffusion constant of water, by integration over time from the relation

$$D = \frac{1}{3} \int_0^{\infty} \langle \vec{v}(t) \cdot \vec{v}(0) \rangle dt. \quad (4.2)$$

The diffusion coefficients, calculated from the mean square displacement and the velocity autocorrelation functions, are displayed in Table IV with the expected errors. The magnitude of the diffusion coefficient of water is much larger in the supercritical region than under ambient conditions, and very long simulations of several hundred picoseconds are required to get reliable results. The percentage error in calculating it is roughly comparable at the two temperatures.

Figure 4 compares the velocity autocorrelation functions

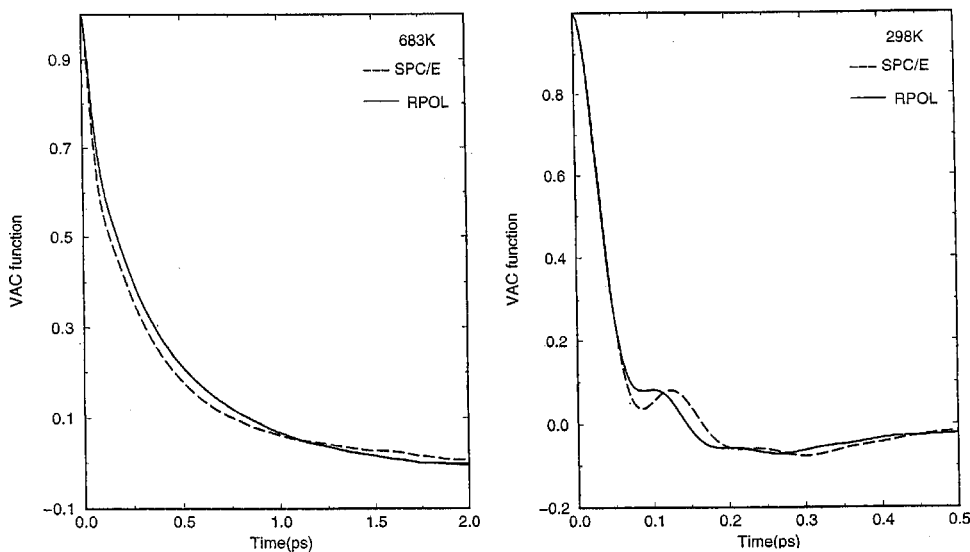


FIG. 4. Comparison between the velocity autocorrelation functions of SPC/E (dashed line) and RPOL (full line) water at 298 K ( $0.997 \text{ g/cm}^3$ ) and 683 K ( $0.350 \text{ g/cm}^3$ ). At 683 K, the velocity autocorrelation function shows a monotonic decay in comparison to the curves at 298 K which oscillate through positive and negative values, indicating that the coordination shell is more loosely held at high temperature.

TABLE IV. Diffusion coefficient of water at 298 K and density of  $0.997 \text{ g cm}^{-3}$  and 683 K at a density of  $0.35 \text{ g cm}^{-3}$  for the SPC/E and RPOL models.

Model Temp	Diffusion constant $D$ ( $10^{-9} \text{ m}^2 \text{ s}^{-1}$ )			
	SPC/E		RPOL	
	MSD	VACI	MSD	VACI
298 K	$2.6 \pm 0.1$	$2.7 \pm 0.1$	$2.5 \pm 0.1$	$2.8 \pm 0.1$
683 K	$99 \pm 4$	$91 \pm 4$	$104 \pm 4$	$98 \pm 4$

of SPC/E and RPOL models at 298 and 683 K. This figure shows that a water molecule oscillates within its first solvation cage at room temperature and a density of  $0.997 \text{ g cm}^{-3}$ . When the temperature is raised to 683 K and the solvent density lowered to  $0.35 \text{ g cm}^{-3}$ , which are typical of the supercritical region, the velocity autocorrelation function decays instead monotonically, indicating that the first solvation shell water molecules, under these conditions, are more loosely held than at room temperature. The basic mechanism of diffusive motion at the two state points appears to be quite different.

## V. RADIAL DISTRIBUTION FUNCTIONS

The ion–oxygen and ion–hydrogen radial distribution functions provide useful information about the equilibrium structure of ions in solution, particularly at infinite dilution when interionic interactions are absent. They provide estimates of the hydration number and size of the hydration shells. The residence time of water in these shells is obtained from an analysis of the residence time correlation function as discussed in the next section. It was noted in the introduction, that the SPC/E and RPOL water models have significant amounts of charge asymmetry and as a result, the orientations of the water molecules in the first solvation shell of a positive and a negative ion are different. For cations like  $\text{Li}^+$  and  $\text{Na}^+$ , the oxygen atoms of water molecules in the first hydration shell are closer to the ion and are pointed to-

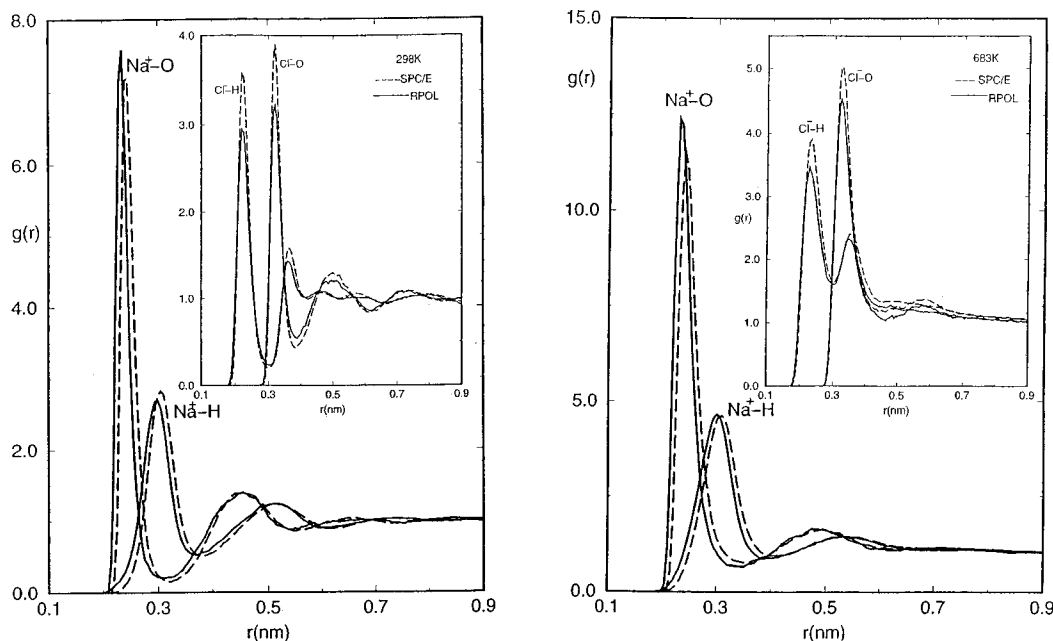


FIG. 5. Ion–oxygen and ion–hydrogen radial distribution functions of  $\text{Na}^+$  and  $\text{Cl}^-$  ion with the RPOL model (full line) and SPC/E model (dashed line) at (a) 298 K and (b) 683 K. For  $\text{Na}^+$ , the distribution functions for the RPOL and SPC/E models are similar, but for the  $\text{Cl}^-$  ion the peak heights predicted by the SPC/E model are slightly higher. The location of the peaks heights are slightly closer to the origin for the RPOL model.

wards it, whereas for a negative ion, such as,  $\text{F}^-$  and  $\text{Cl}^-$  one of the hydrogen atoms of a water molecule in this shell is closer than the oxygen atom of the same water molecule and is pointed towards the ion. This helps to understand the main features of the distribution functions.

Figure 5 shows the ion–oxygen and ion–hydrogen radial distribution functions for  $\text{Na}^+$  and  $\text{Cl}^-$  at 298 K and 683 K using the RPOL and SPC/E models for water. The positive  $\text{Na}^+$  ion, shows two prominent solvation shells whereas the negative  $\text{Cl}^-$  ion, exhibits three shells as discerned from the ion–oxygen distribution functions. The locations and heights of these peaks, in the RPOL model are in close proximity to the corresponding peaks for the same ion in SPC/E water, but slightly closer to the origin for the RPOL model on account of the electronic polarization of the ions and water molecules. However, the peak heights for the  $\text{Cl}^-$  ion in SPC/E model are significantly higher than what they are for the RPOL model, although the locations of the peaks are only slightly affected. The opposite is true for the peak heights of the cations, although the differences between the two models are small.

Figure 6 shows the ion–oxygen and ion–hydrogen radial distribution functions for  $\text{Li}^+$  and  $\text{F}^-$  at 298 K and 683 K, using the RPOL and SPC/E models. The  $\text{Li}^+$  ion is the smallest of the ions studied and has the lowest polarizability.

The small size implies a strong electric field at the surface capable of polarizing the surrounding water more strongly than the other ions. The fluoride ion is intermediate in size between  $\text{Na}^+$  and  $\text{Cl}^-$ , and carries an atomic polarizability that also lies between the values for these two ions. These figures reveal the same features as for  $\text{Na}^+$  and  $\text{Cl}^-$ , with higher peaks in the oxygen and hydrogen ion distribution functions for the negative  $\text{F}^-$  ion in SPC/E water than in RPOL water. The positions of the peaks in the distribution

functions for the RPOL model are shifted slightly towards the origin in proportion to the polarizabilities of the ion and oxygen or hydrogen of water closest to it.

The hydration numbers in the first shell, were calculated from the integral

$$N_h = \rho_w \int_0^{R_U} g_{iO}(r) 4\pi r^2 dr, \quad (5.1)$$

where  $R_U$  is the radius of the hydration shell given by the position of the first minimum in the ion–oxygen radial distribution function  $g_{iO}(r)$  and  $\rho_w$  is the number density of water. The results are summarized in Table V. We see the hydration numbers of the ions for both models are nearly the same and are insensitive to the change in temperature and

TABLE V. Hydration numbers and residence times of water in the primary solvation shells of ions and bulk water.

Temperature	298 K	683 K	
Solvent density	0.997 g cm <sup>-3</sup>	0.35 g cm <sup>-3</sup>	
Ion	Water model	Hydration number (residence time in ps)	
$\text{Li}^+$	SPC/E	4.1(51)	4.0(9)
	RPOL	3.8(>150)	3.9(8)
$\text{Na}^+$	SPC/E	5.8(20)	4.9(3)
	RPOL	5.3(29)	5.2(3)
$\text{F}^-$	SPC/E	6.3(24)	6.1(2)
	RPOL	5.7(29)	5.6(2)
$\text{Cl}^-$	SPC/E	7.2(13)	7.1(3)
	RPOL	6.9(12)	7.4(2)
Water	SPC/E	4.4(5)	4.1(–) <sup>a</sup>
	RPOL	4.2(5)	4.6(–) <sup>a</sup>

<sup>a</sup>The residence time of water in its first coordination shell at a solvent density of 0.35 g cm<sup>-3</sup> and temperature of 683 K is too small to determine accurately.

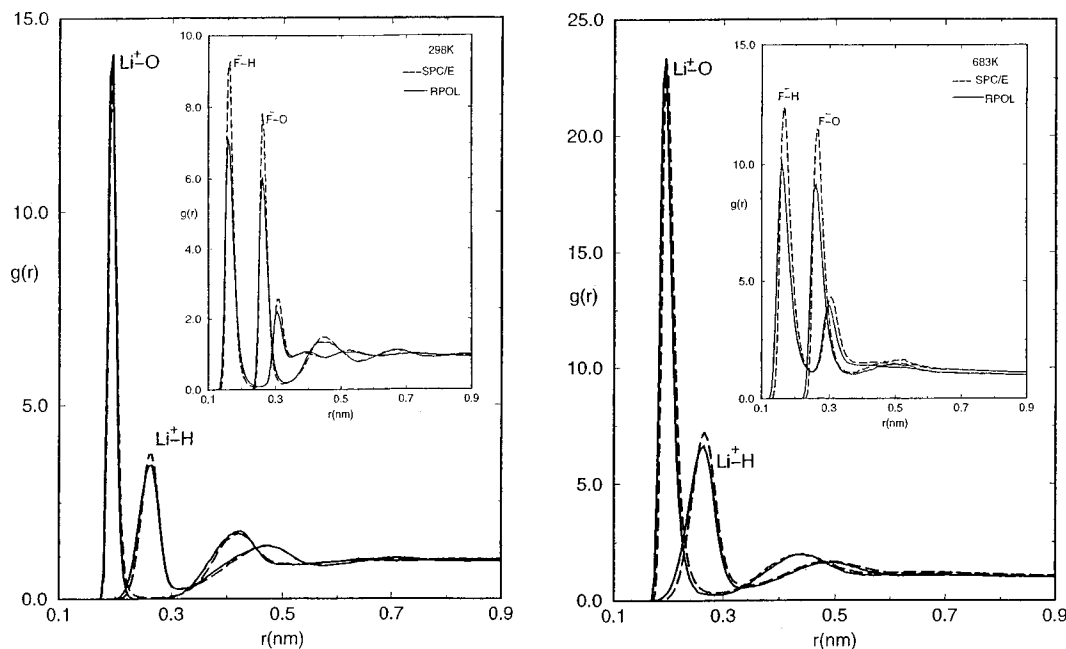


FIG. 6. Ion–oxygen and ion–hydrogen radial distribution functions of  $\text{Li}^+$  and  $\text{F}^-$  ions with RPOL model (full line) and SPC/E model (dashed line) at (a) 298 K and (b) 683 K. For the  $\text{Li}^+$  ion, the distribution functions for the ion in RPOL water and SPC/E water are similar, but for the  $\text{F}^-$  ion, the peak heights in RPOL model are slightly lower at 298 K and 683 K than in SPC/E model for water.

solvent density from  $0.997 \text{ g cm}^{-3}$  at 298 K to  $0.35 \text{ g cm}^{-3}$  at 683 K. Although the structure of the primary hydration shell of an ion in the two states are the same, the dynamics of these shells may be different and are discussed next.

## VI. RESIDENCE TIME CORRELATION FUNCTIONS

The residence times were calculated from the time correlation function defined by

$$R(t) = \frac{1}{N_h} \sum_{i=1}^{N_h} \langle \theta_i(t) \theta_i(0) \rangle. \quad (6.1)$$

Here  $\theta_i(t)$  is the Heaviside unit step function, which is 1 if a water molecule is in the coordination shell of the ion at  $t$  and zero otherwise, and  $N_h$  is the hydration number of this shell. We allow for a temporary excursion time of 2 ps at room temperature, by treating a water molecule to be present in the first solvation shell, if it returns back within this time. At the supercritical temperature of 683 K however, no allowance for this type excursion was made, because of the rapid exchange of water between the shell and the bulk. The residence time  $\tau$  of water in the hydration shell of an ion was calculated from the integral of the residence time correlation function:

$$\tau = \int_0^{\infty} R(t) dt. \quad (6.2)$$

The details of the integration procedure are described elsewhere.<sup>5–8</sup> The residence times of the ions at 298 K and 683 K are displayed in Table V from which it is evident that they differ by an order of magnitude at the two temperatures for both the SPC/E and RPOL water models. We recall that in our studies, the density of water at 298 K is  $0.997 \text{ g cm}^{-3}$  and at 683 K it is  $0.35 \text{ g cm}^{-3}$ .

Figure 7 shows the residence time correlation function for the  $\text{Na}^+$  and  $\text{Cl}^-$  ions at supercritical and room temperatures. The residence time of water in the first solvation shell of  $\text{Na}^+$  ion at room temperature (Table V) is greater in the RPOL model than for the SPC/E model while they are equal at the elevated temperature of 683 K. For the  $\text{Cl}^-$  ion, the residence times are more nearly the same for the two models at both temperatures, within the error of our simulations which is about 2 ps at 298 K and 0.5 ps at 683 K. The same trend is also present for the small ions  $\text{Li}^+$  and  $\text{F}^-$ . This is shown in Fig. 8.

For the  $\text{Li}^+$  ion at room temperature, polarization causes its residence time to be very large in the RPOL model, showing that this model predicts that the ion moves with its solvation cage. This is the extreme example of the “solvent-burg” model of ion mobility. When the temperature is increased to 683 K, electrostatic interactions between the ion and its solvent cage are greatly reduced and the residence time decreases. In contrast to  $\text{Li}^+$ , the residence time of water in the first hydration shell of the larger negative  $\text{F}^-$  ion is less affected by the polarization of the ion and solvent inherent in the RPOL model.

## VII. SOLVENT POLARIZABILITY AND THE DIFFUSION COEFFICIENT OF IONS IN AQUEOUS SOLUTIONS AT INFINITE DILUTION

In this section we investigate the effect of solvent electronic polarization on the diffusion coefficients of monovalent ions ( $\text{Na}^+$ ,  $\text{Li}^+$ ,  $\text{Cl}^-$ , and  $\text{F}^-$ ), at ambient and supercritical temperatures. Our previous studies, using the SPC/E model for water, showed that the diffusion of ions of group one and seven, lie on two separate curves at room temperature with each passing through a maximum, when plotted

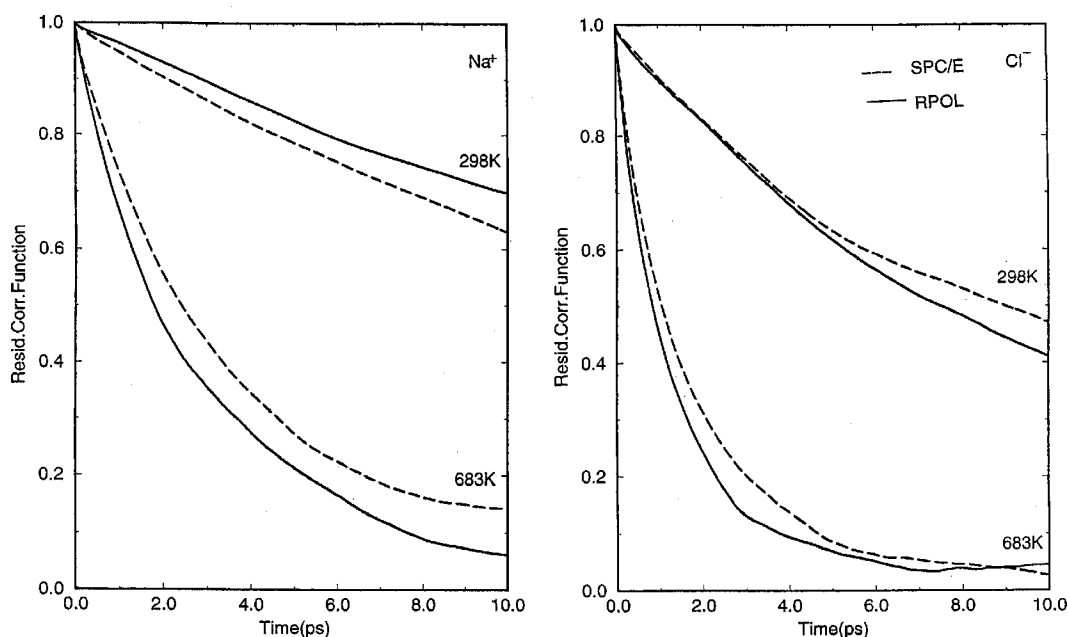


FIG. 7. Residence time correlation function for  $\text{Na}^+$  (left) and  $\text{Cl}^-$  (right) ions at 298 K and 683 K with SPC/E (dashed line) and RPOL (full line) models. Note that the difference between the models is small for the larger negatively charged  $\text{Cl}^-$ .

against ion size.<sup>4-6</sup> We now turn to a discussion of the diffusion coefficients of these ions at 298 K and 683 K using the SPC/E and RPOL models for water. Our results are summarized in Table VI.

Examining Fig. 9, one sees that the long time slopes of the MSD curves for the  $\text{Na}^+$  and  $\text{Cl}^-$  ions are not affected by whether one uses the RPOL or SPC/E model for water. Thus polarizability of the ions and the solvent makes little difference to the diffusion coefficients of  $\text{Na}^+$  and  $\text{Cl}^-$  ion at ambient and elevated temperatures.

This is confirmed by the velocity autocorrelation (VAC) functions presented in Fig. 10, which also shows small differences between the two models and leads, on integration, to diffusion coefficients for the ions that are essentially the same for both models of water.

Another observation is that the velocity autocorrelation functions of the  $\text{Na}^+$  and  $\text{Cl}^-$  ions at 683 K are never nega-

tive during their descent to zero, but show characteristic oscillations through positive and negative regions in their decay to zero at 298 K. This implies that the oscillation of the ion in its solvent cage at 298 K is absent at high temperatures. This is consistent with the shorter residence time of the hydration shells of these ions at elevated temperatures. The situation is different for the  $\text{Li}^+$  ion discussed below.

The smaller size of  $\text{Li}^+$  and  $\text{F}^-$  causes the effective field in their immediate vicinity to be greater than what it is for larger ions such as  $\text{Na}^+$  and  $\text{Cl}^-$ . The field polarizing the surrounding water molecules may lead to additional reorientation of the water of hydration. The orientations of the water molecules in the hydration shells of positive and negative ions are, as noted earlier, very different especially for small ions for which the hydration shells are held together by ion-solvent electrostatic interactions. Table V shows that the residence times of water in the hydration shell of the  $\text{Li}^+$  ion is much larger than the residence time of water in the hydration shell of the fluoride ion.

Figure 11 shows the mean square displacement of  $\text{Li}^+$  and  $\text{F}^-$  at ambient and supercritical temperatures. An interesting observation is that at 298 K the slope of the MSD of the  $\text{Li}^+$  in RPOL water is less than the corresponding slope for  $\text{Li}^+$  in SPC/E water, which translates into a decrease in the diffusion coefficient for the polarizable  $\text{Li}^+$  ion at 298 K. Bear in mind that the polarizability of the  $\text{Li}^+$  ion itself is small ( $0.029 \text{ \AA}^3$ ), but its polarizing power is large by virtue of the intense electric field in its vicinity. On the other hand, the polarizability of the  $\text{F}^-$  ion ( $0.974 \text{ \AA}^3$ ) is much larger than the polarizability of the  $\text{Li}^+$  ion, but its polarizing power is weaker since it is larger than the  $\text{Li}^+$  ion. The slope of the MSD of  $\text{F}^-$  in RPOL at 298 K is essentially the same as the corresponding slope in SPC/E water. However, at 683 K and a solvent density of  $0.35 \text{ g cm}^{-3}$ , the differences in the slopes of the mean square displacement curve of the  $\text{Li}^+$  for

TABLE VI. Diffusion coefficients of ions at infinite dilution in SPC/E and RPOL water at 298 K and density of  $0.997 \text{ g cm}^{-3}$  and 683 K at a density of  $0.35 \text{ g cm}^{-3}$ . The uncertainties in the diffusion coefficients are nearly the same for the other ions as for  $\text{Li}^+$  at each temperature and solvent density.

Temperature Solvent density	Diffusion constant $D(10^{-9} \text{ m}^2 \text{ s}^{-1})$			
	298 K $0.997 \text{ g cm}^{-3}$		683 K $0.35 \text{ g cm}^{-3}$	
	MSD	VACI	MSD	VACI
$\text{Li}^+$ (SPC/E)	$1.2 \pm 0.1$	$1.2 \pm 0.1$	$30 \pm 2$	$30 \pm 2$
(RPOL)	$0.9 \pm 0.1$	$0.9 \pm 0.1$	$32 \pm 2$	$30 \pm 2$
$\text{Na}^+$	1.3	1.3	32	34
	1.4	1.3	32	33
$\text{F}^-$	1.0	1.0	36	35
	0.9	0.8	30	30
$\text{Cl}^-$	1.8	1.7	37	37
	1.7	1.6	37	36

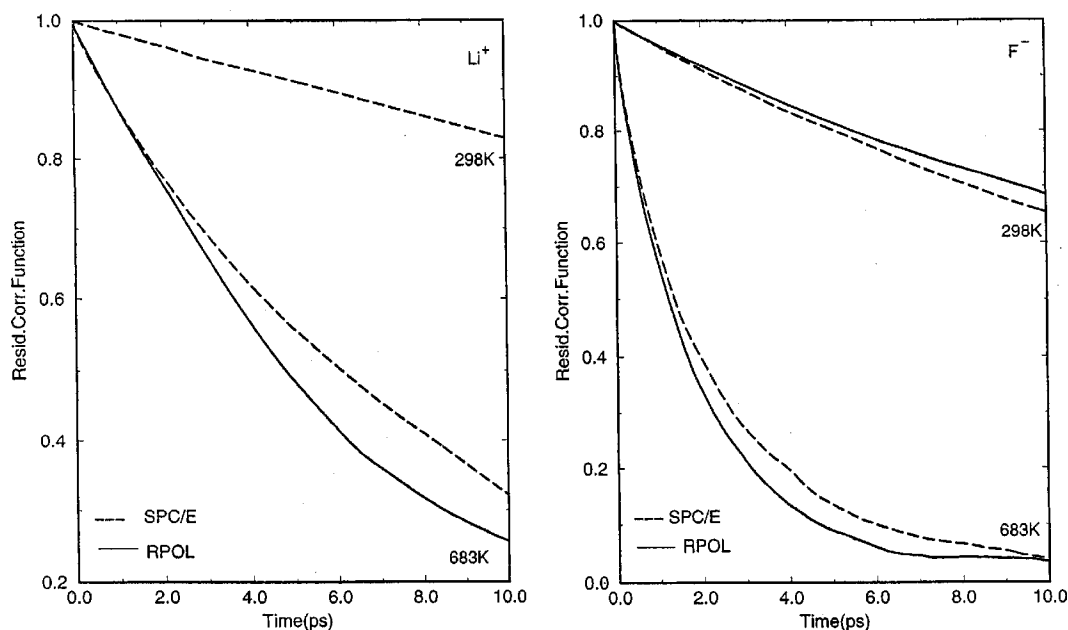


FIG. 8. Residence time correlation function for  $\text{Li}^+$  (left) and  $\text{F}^-$  (right) at 298 K and 683 K with SPC/E (dashed line) and RPOL (full line) models. For the  $\text{Li}^+$  ion the RPOL model predicts a very large residence time at 298 K and the residence time correlation function on this scale is essentially coincident with the abscissa. At 683 K, the residence time correlation function of the water of hydration of the  $\text{Li}^+$  ion in the RPOL model lies below the corresponding curve for SPC/E water at intermediate times.

the two models is small, taking into account the larger errors at high temperature (see Table VI). This suggests that ion and solvent polarizability plays a less important role in the diffusion of  $\text{Li}^+$  ions at elevated temperatures at infinite dilution. For the  $\text{F}^-$  ion however, our studies show a slight decrease in the diffusion coefficient of this ion at the 683 K state point on changing from the SPC/E to the RPOL model. This suggests that ion and solvent polarizability may play a more important role for  $\text{F}^-$  than for  $\text{Li}^+$ .

Figure 12 shows the velocity autocorrelation functions for the  $\text{Li}^+$  and  $\text{F}^-$  ions, at 298 and 683 K. At room tem-

perature, polarization effects cause a decrease in the amplitude of the oscillations of the ion velocity autocorrelation functions at short times for the  $\text{F}^-$  ion, but leaves the corresponding functions for the  $\text{Li}^+$  ion less affected. The  $\text{Li}^+$  is anomalous in that it is the only one of the ions studied so far whose velocity autocorrelation functions shows pronounced oscillations that pass through negative values at 683 K. This is consistent with the larger residence time of the solvation cage of  $\text{Li}^+$  ion at this temperature and indicates that the ion oscillates in its solvent cage even at supercritical temperatures when either of the SPC/E and RPOL models are used to

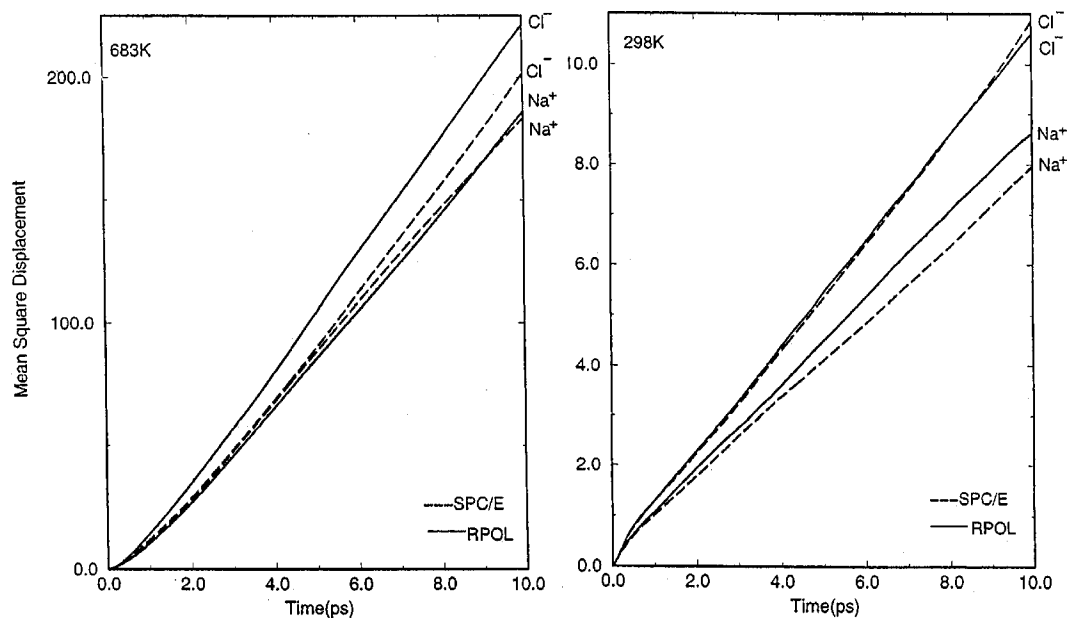


FIG. 9. Mean square displacement of  $\text{Na}^+$  and  $\text{Cl}^-$  in  $\text{\AA}^2$  at 298 K and 683 K calculated for the SPC/E (dashed line) and RPOL (full line) models.

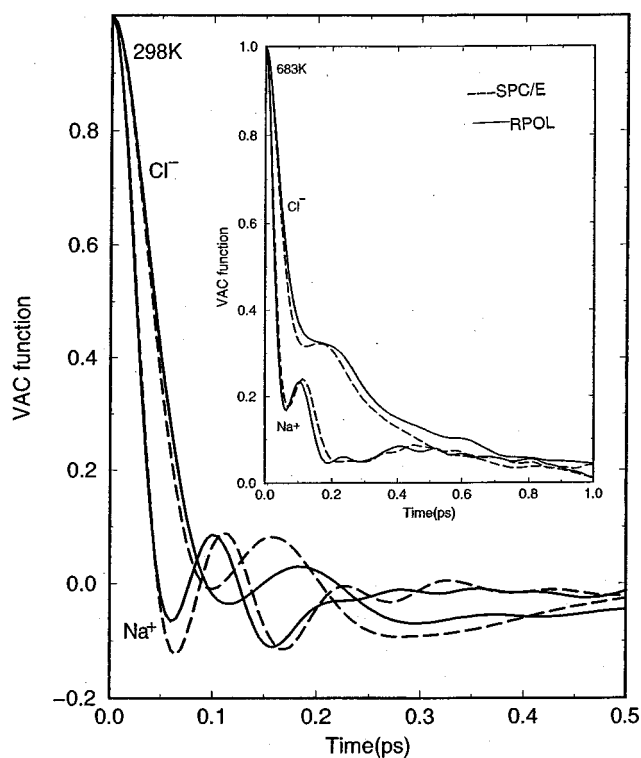


FIG. 10. Velocity autocorrelation function of  $\text{Na}^+$  and  $\text{Cl}^-$  at 298 K and 683 K (inner subset) with SPC/E (dashed line) and RPOL (solid line) models. The differences for the same ion are larger at 298 K than at 683 K.

represent the solvent water. At a supercritical temperature of 683 K, the  $\text{F}^-$  and  $\text{Li}^+$  velocity autocorrelation functions are also not changed significantly by the introduction of ion and solvent atom polarizability in the RPOL model.

These studies show that the diffusion coefficients of ions in infinite dilute aqueous solution at a solvent density of  $0.35 \text{ g cm}^{-3}$  and temperature of 683 K are an order of magnitude

greater, and only weakly dependent on the size of the ions<sup>7,8</sup> in contrast to their behavior under ambient conditions.<sup>5</sup> This is independent of whether the SPC/E or RPOL model is used for water.

## VIII. DISCUSSION AND CONCLUSION

Even though the hydrogen-bonding peak of the O–H distribution function is affected by the polarization at supercritical temperatures, the impact of polarization on the diffusion coefficient of water, is small within the errors of our simulations. Figures 1 and 2 clearly show that there are small differences in the extent of hydrogen bonding for both models, and polarization in the RPOL model slightly favors higher hydrogen bonding at room temperature but much less so at elevated temperatures.

A cation has the oxygen atom of a water molecule in its first hydration shell closer to it than the hydrogen atoms of the same molecule, and this oxygen atom is polarized especially by small ions like  $\text{Li}^+$  and  $\text{Na}^+$ . In the case of negative ions like  $\text{F}^-$  and  $\text{Cl}^-$ , one of the hydrogen atoms of the water of hydration is closer to the ion than the oxygen atom of the same water molecule. The polarizability of the hydrogen is smaller than that of the oxygen atom and is equal to about half its value (see Table II). The differences in the peak heights of the ion–oxygen and ion–hydrogen distribution functions for negative ions can be traced to the differences in the treatment of electronic polarization in the SPC/E and RPOL models. As the size of the ion increases, the field at its surface decreases causing less polarization of the surrounding atoms in the RPOL model. The peak heights of the ion–hydrogen distribution functions of the negative ions are however lower for the RPOL model than they are for the SPC/E model. This may be related to the smaller charge on the hydrogen atoms of water in the RPOL model than in the SPC/E model, which is only partly compensated by the large

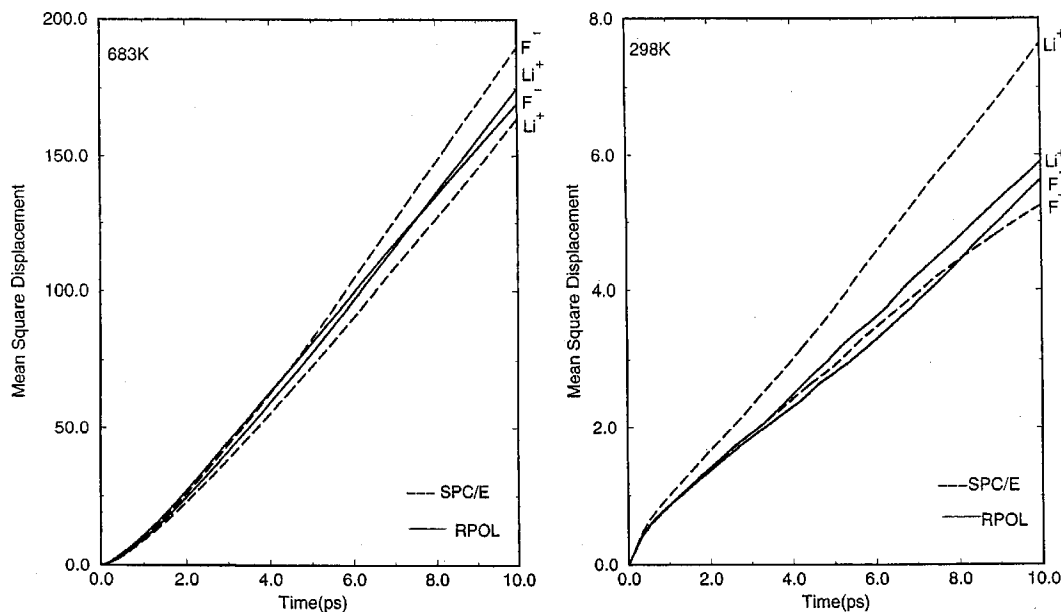


FIG. 11. The mean square displacements of  $\text{Li}^+$  and  $\text{F}^-$  in  $\text{\AA}^2$  at 298 K and 683 K calculated for the SPC/E (dashed line) and RPOL (full line) models for water.

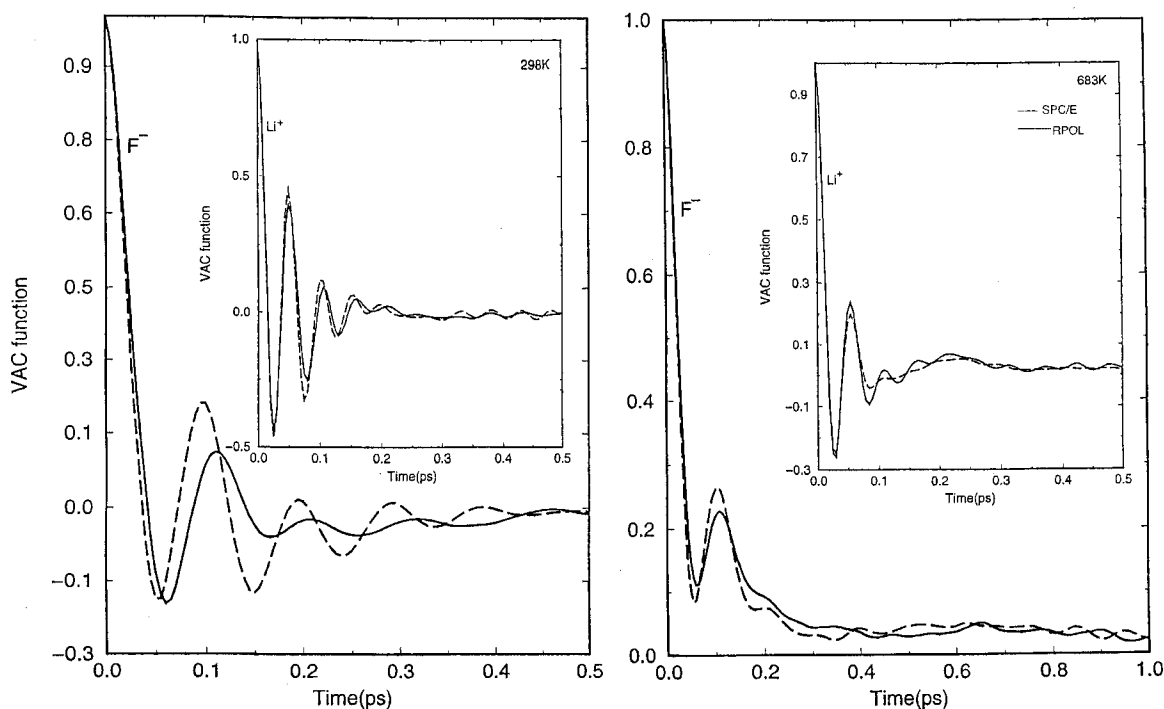


FIG. 12. Comparison between the velocity autocorrelation function of  $\text{Li}^+$  and  $\text{F}^-$  at 298 K and 683 K with SPC/E (dashed line) and RPOL (full line) models for water. Other than the  $\text{F}^-$  ions at 298 K, both models show a very close behavior.

polarizability of the small negative ions in the RPOL model—see Tables I and II. This clearly suggests that polarization effects on the structure of ions in infinitely dilute solutions may be important for small ions, with the positive ions more affected than the negatively charged ions. The situation may be altered in concentrated electrolyte solutions in which the ion–ion interactions cannot be ignored.

Examining Table V we see that the coordination numbers in the first hydration shell, for both models at both temperatures are nearly the same. However, the decrease in the residence time spent by the water molecules (summarized also in Table V) in the first solvation shells at 683 K suggests significant exchange of water between the first solvation shell and the surrounding water at elevated temperatures. The residence time of the water of hydration in the primary shell of the  $\text{Li}^+$  ion at 298 K is extremely large (essentially infinite on a picosecond time scale) in the RPOL model, in comparison to the residence time of  $\approx 51$  ps in SPC/E water. This increase is also observed in the residence times of small cations and anions, e.g.,  $\text{Na}^+$  and  $\text{F}^-$  when the RPOL model is used to model water. Elevated temperatures (683 K) cause the effects of polarization to decrease, and the residence time of water molecules around small positive and negative ions is lower than at 298 K ions and less sensitive to the model used for water (SPC/E or RPOL).

An important conclusion is that the explicit neglect of polarizability and its temperature dependence in the SPC/E model does not lead to serious errors in the interpretation of the structure and dynamics of infinitely dilute aqueous, at supercritical and room temperatures. Possible exceptions are the smallest ions ( $\text{F}^-$  and  $\text{Li}^+$ ), but here again atomic polarizability represented in the RPOL model has only a small

effect on the diffusion coefficients and hydration numbers of these ions at 298 K and 683 K.

We note that the velocity autocorrelation functions of the ions, except  $\text{Li}^+$ , are always positive at 683 K and a solvent density of  $0.35 \text{ g cm}^{-3}$ , whereas they oscillate through positive and negative values while decaying to zero with time at 298 K and a solvent density of  $0.997 \text{ g cm}^{-3}$ . This suggests that the mechanism of diffusion of these ions in the supercritical state studied may be quite different to what it is at ambient conditions. The solvent is highly compressible in supercritical states, and the mechanism of solute diffusion in this region could also be sensitive to the solvent density. It would be of interest to extend studies<sup>28–30</sup> of hydrogen bond dynamics in water to supercritical and ambient temperatures using the SPC/E or RPOL models.

## ACKNOWLEDGMENTS

This study was supported by Grant No. CHE 9961336 to J.C.R. from the National Science Foundation. S.K. thanks the Pacific National Laboratory for a visiting student fellowship and for their hospitality. Part of the study was performed in the Environmental Molecular Sciences Laboratory (EMSL) at the Pacific Northwest National Laboratory under the auspices of the Division of Chemical Sciences, Office of Basic Energy Sciences, U.S. Department of Energy. Computer resources were provided by the Division of Chemical Sciences and by the Scientific Computing Staff, Office of Energy Research, at the National Energy Research Super-

computer Center (Berkley, California). The operation of EMSL is supported by DOE's office of Biological and Environmental Research.

- <sup>1</sup>L. X. Dang, Chem. Phys. Lett. **200**, 21 (1992); L. X. Dang and B. C. Garrett, J. Chem. Phys. **99**, 2972 (1993); L. X. Dang and P. Kollmann, J. Phys. Chem. **99**, 55 (1995); L. X. Dang, J. Am. Chem. Soc. **117**, 6954 (1995); L. X. Dang, J. Chem. Phys. **102**, 3483 (1995).
- <sup>2</sup>L. X. Dang, J. Chem. Phys. **97**, 2659 (1992); **96**, 6970 (1992); **100**, 3757 (1994); **96**, 6970 (1992).
- <sup>3</sup>R. M. Lynden-Bell and J. C. Rasaiah, J. Chem. Phys. **107**, 1981 (1997).
- <sup>4</sup>S. H. Lee and J. C. Rasaiah, J. Phys. Chem. **100**, 1420 (1996).
- <sup>5</sup>S. Koneshan, J. C. Rasaiah, R. M. Lynden-Bell, and S. H. Lee, J. Phys. Chem. **102**, 4193 (1998).
- <sup>6</sup>S. Koneshan, R. M. Lynden-Bell, and J. C. Rasaiah, J. Am. Chem. Soc. **120**, 12041 (1998).
- <sup>7</sup>J. C. Rasaiah, J. P. Noworyta, and S. Koneshan, J. Am. Chem. Soc. **122**, 11182 (2000).
- <sup>8</sup>J. P. Noworyta, S. Koneshan, and J. C. Rasaiah, J. Am. Chem. Soc. **122**, 11193 (2000).
- <sup>9</sup>S. Koneshan and J. C. Rasaiah, J. Chem. Phys. **113**, 8125 (2000).
- <sup>10</sup>S. H. Lee and P. T. Cummings, J. Chem. Phys. **112**, 864 (2000).
- <sup>11</sup>H. J. C. Berendsen, J. R. Grigera, and T. P. Straatsma, J. Phys. Chem. **91**, 6269 (1987).
- <sup>12</sup>A. K. Soper, F. Bruni, and M. A. Ricci, J. Chem. Phys. **106**, 247 (1997); A. K. Soper, J. Phys.: Condens. Matter **9**, 2717 (1997).
- <sup>13</sup>A. A. Chialvo and P. T. Cummings, J. Phys. Chem. **100**, 1309 (1996); J. Chem. Phys. **101**, 4466 (1994).
- <sup>14</sup>D. E. Smith and L. X. Dang, J. Chem. Phys. **100**, 3757 (1994).
- <sup>15</sup>P. B. Balbuena, K. P. Johnson, and P. J. Rossky, J. Phys. Chem. **100**, 2706 (1996); **100**, 2705 (1996); P. B. Balbuena, K. P. Johnston, and P. J. Rossky, and J. K. Hyun, J. Phys. Chem. **102**, 3806 (1998); P. J. Rossky and K. P. Johnson, in *Steam, Water and Hydrothermal Systems: Physics and Chemistry Meeting the Needs of Industry*, Proceedings of the 13th International Conference on the Properties of Water and Steam, edited by P. R. Tremaine, P. G. Hill, D. G. Irish, and P. V. Balakrishnan (NRC Research Press, Canada, 2000), p. 131.
- <sup>16</sup>J. W. Tester, P. A. Marron, M. M. DiPippo, K. Sako, M. T. Reagan, T. Arias, and W. A. Peters, J. Supercrit. Fluids **13**, 225 (1998); T. Driesner, T. M. Seward, and I. G. Tironi, Geochim. Cosmochim. Acta **62**, 3095 (1998).
- <sup>17</sup>R. Fernández-Prini and M. L. Japas, Chem. Soc. Rev. **23**, 155 (1994).
- <sup>18</sup>E. H. Oelkers and H. C. Helgeson, Science **261**, 888 (1993).
- <sup>19</sup>O. Kajimoto, Chem. Rev. **99**, 355 (1999).
- <sup>20</sup>S. C. Tucker, Chem. Rev. **99**, 391 (1999); S. C. Tucker and M. W. Maddox, J. Phys. Chem. B **102**, 2437 (1998).
- <sup>21</sup>R. Mountain, J. Chem. Phys. **103**, 3084 (1995).
- <sup>22</sup>N. Yoshii, H. Yoshie, S. Miura, and S. Okazaki, J. Chem. Phys. **109**, 4873 (1998).
- <sup>23</sup>A. Wallquist and R. D. Mountain, in *Reviews in Computational Chemistry*, edited by K. B. Lipkowitz and D. B. Boyd (Wiley-VCH, Wiley, New York, 1999), Vol. 13, Chap. 4.
- <sup>24</sup>S. W. Rick, J. Chem. Phys. **114**, 2276 (2001), and references therein.
- <sup>25</sup>P. L. Silvestrelli and M. Parrinello, Phys. Rev. Lett. **82**, 3308 (1999).
- <sup>26</sup>L. Delle Sitte, A. Alavi, and R. M. Lynden-Bell, Mol. Phys. **96**, 1683 (1999).
- <sup>27</sup>B. D. Bursalaya and H. J. Kim, J. Chem. Phys. **109**, 4911 (1998); **110**, 9656 (1999), and references therein; C. Yang and H. J. Kim, *ibid.* **113**, 6025 (2000).
- <sup>28</sup>A. Luzar and D. Chandler, Nature (London) **379**, 55 (1996).
- <sup>29</sup>A. Luzar and D. Chandler, Phys. Rev. Lett. **76**, 928 (1996).
- <sup>30</sup>A. Luzar, J. Chem. Phys. **113**, 10663 (2000).